Evidence for vesicles that mediate long-chain fatty acid uptake by human microvascular endothelial cells

Axel Ring,[1,*] Jürgen Pohl,[*] Alfred Völkl,[†] and Wolfgang Stremmel[2,*]

Department of Internal Medicine IV* and Department of Anatomy and Cell Biology,[†] Ruprecht-Karls-University, Heidelberg, Germany

Abstract **This study analyzes the mechanisms of long-chain fatty acid (LCFA) uptake by human microvascular endothelial cells (HMEC). The time course revealed the presence of an early, carrier-mediated uptake component and a later component mediated by clathrin-coated vesicles (CCV) and caveolae, as evidenced by three different experimental approaches: *1*) significant reduction of [^{3}H]oleate uptake over 5 min by either inhibition of CCV formation by potassium depletion or hypertonic medium, or disruption of caveolae by filipin III or cyclodextrin. *2*) Co-localization of intracellular 12-(*N*-methyl)-*N*-[(7-nitrobenz-2-oxa-1,3-diazol-4-yl)amino]octadecanoic acid with CCV and caveolae using confocal laser scanning microscopy. *3*) Enrichment of [^{3}H]oleate in a subcellular fraction containing CCV and caveolae. Within 10 min, more than 75% of intracellular [^{3}H]oleate remained unmetabolized, suggesting that HMEC preferentially shuttle LCFA through the cell using CCV and caveolae as carriers. The uptake of albumin paralleled that of oleate within the first 10 min, suggesting internalization of at least some LCFA bound to albumin. Compared to oleate and albumin, the uptake of sucrose and dextran was low, indicating a potential minor contribution of fluid-phase endocytosis to the total vesicular LCFA uptake. The data indicate a previously unrecognized role of both CCV and caveolae for the uptake of LCFA by HMEC.**—Ring, A., J. Pohl, A. Völkl, and W. Stremmel. **Evidence for vesicles that mediate long-chain fatty acid uptake by human microvascular endothelial cells. *J. Lipid Res.* 2002.** 43: **2095–2104.**

Supplementary key words clathrin-coated vesicles • caveolae • clathrin-coated vesicles

Long-chain fatty acids (LCFA) are physiologically important molecules as energy substrates and as precursors for the synthesis of membrane lipids or lipid mediators (such as prostaglandins, leukotrienes, and thromboxane) (1, 2). In addition, LCFA mediate crucial cellular processes, such as control of cell differentiation, cell signalling, and regulation of gene transcription (3). As most tissues have limited or no capacity to synthesize LCFA on their own, they depend on LCFA uptake from the circulation. Both the liver and the heart are extremely efficient in extracting LCFA from the blood (1, 4). The endothelial layer is the first barrier to be traversed by LCFA before they can be metabolized by the underlying parenchymal tissue. LCFA circulate in the blood as albumin-bound complexes or in chylomicrons (from intestinal absorption) or lipoproteins (from hepatic synthesis). The latter two are hydrolyzed by endothelial lipoprotein lipase resulting in the generation of free LCFA, which are rapidly bound by albumin due to their low solubility in aqueous solutions. In a rat model, LCFA from blood-borne LDLs were found inside liver endothelial cells and were rapidly transferred to the hepatocytes (5). This indicates that LCFA uptake across the luminal membrane of endothelial cells is a crucial step in the process of fatty acid transport from blood to tissue. However, while LCFA uptake by hepatocytes (6), adipocytes (7), cardiomyocytes (8), and intestinal mucosal cells (9) is well characterized and known to be mediated by protein-facilitated transport, our knowledge of the mechanisms underlying LCFA uptake into endothelial cells is sketchy.

In the present study, we studied the uptake of [^{3}H]oleate and 12-(*N*-methyl)-*N*-[(7-nitrobenz-2-oxa-1,3-diazol-4-yl)amino]stearate (12-NBD) into human microvascular endothelial cells (HMEC) by *a*) the effects of inhibitors of carrier-mediated and vesicle-associated uptake, *b*) confocal laser scanning microscopy (LSM), and *c*) by subcellular fractionation of HMEC following uptake of [^{3}H]oleate. We propose that LCFA uptake into HMEC is a two-component process involving both a high-affinity, low capacity protein-facilitated mechanism and a high-capacity vesicle-mediated component.

Abbreviations: CCV, clathrin-coated vesicles; FAT, fatty acid translocase, HMEC, human microvascular endothelial cells; LCFA, long-chain fatty acids; LSM, laser scanning microscopy; 12-NBD, stearate 12-(*N*-methyl)-*N*-[(7-nitrobenz-2-oxa-1,3-diazol-4-yl)amino]stearate; NEM, *N*-ethylmaleimide.

[1] A. Ring and J. Pohl contributed equally to this work.

[2] To whom correspondence should be addressed.
e-mail: wolfgang_stremmel@med.uni-heidelberg.de

Manuscript received 19 July 2002 and in revised form 11 September 2002.

Published, JLR Papers in Press, September 16, 2002.
DOI 10.1194/jlr.M200285-JLR200

MATERIALS AND METHODS

Materials

12-NBD stearate was obtained from Molecular Probes (Eugene, OR). [^{3}H]oleate (60 Ci/mmol; 1 Ci = 37 GBq) was from Biotrend (Cologne, Germany). Fatty acid-free BSA (fraction V), filipin III, cyclodextrin, *N*-ethylmaleimide, monensin, phloretin, and non-radioactive oleate were purchased from Sigma Chemical (St. Louis, MO). Ultima Gold scintillation fluid was from Packard (Groningen, The Netherlands). The murine monoclonal antibody against caveolin-1 was from Transduction Laboratories (Lexington, KY), the polyclonal antibody against clathrin-heavy chain was a kind gift from Dr. Margaret Robinson from the Cambridge Institute for Medical Research (Cambridge, UK). The secondary antibodies were obtained from Sigma Chemical. The Western blots were detected using the ECL reagents (Amersham, Little Chalfont, England).

Cell culture

The HMEC-1 cell line (10) was kindly provided by Francisco J. Candal of the Centers for Disease Control and Prevention, Atlanta, GA. This cell line had previously been validated as a model system for cholesterol uptake (11). The cells were grown to confluence in EBM medium (Clonetics) supplemented with 5% fetal calf serum and the EBM Bullet Kit (Clonetics).

Assay of [^{3}H]oleate uptake

The [^{3}H]oleate uptake assays were performed as described previously (6) using confluent HMEC-1 monolayers in 5 cm ø culture dishes. The concentrations of unbound fatty acids in [^{3}H]oleate-BSA solutions (fixed BSA concentration = 173 μmol/l, oleate:BSA molar ratios ranging from 0.1 to 2) were calculated by the stepwise equilibrium constant of Wosilait and Nagy (12), using the dissociation constants for the oleate-albumin complex reported by Spector et al. (13).

For the concomitant determination of albumin uptake, trace amounts of [methyl-^{14}C]BSA (Biotrend, Cologne, Germany) were added to the 173 μmol/l oleate:BSA solution.

[^{3}H]oleate uptake inhibition studies

Various inhibitors were used to pretreat HMEC prior to incubation with [^{3}H]oleate bound to albumin as described above. The following substances were used:

Substance	Concentration
Phloretin	400 μmol/l in PBS-1%BSA
N-ethymaleimide (NEM)	1 mmol/l in PBS-1%BSA
Monensin	30 μmol/l in PBS-1%BSA
K^+ depletion	140 mM NaCl, 1 mM $CaCl_2$, 1 mM $MgCl_2$, 10 mM HEPES, 5.5 mM glucose, 1% BSA
Hypertonic medium	350 mM NaCl, 1 mM $CaCl_2$, 1 mM $MgCl_2$, 10 mM HEPES, 5.5 mM glucose, 1% BSA
Cyclodextrin	10 mmol/l
Filipin III	2.5 mmol/l in PBS-1%BSA

Assay of [^{3}H]dextran, [^{3}H]sucrose, and ^{125}I-transferrin uptake

Confluent HMEC-1 monolayers in 5 cm ø culture dishes were incubated with 5 mg/ml dextran (average molecular weight 70,000; Sigma, St. Louis, MO) or 100 μmol/l sucrose and trace amounts of [^{3}H]dextran (molecular weight 70,000; Biotrend, Cologne, Germany) or [^{3}H]sucrose (Pharmacia Biotech, Little Chalfont, UK), respectively, in 2 ml of PBS at 37°C for 10, 20, or 30 min. Subsequently, the monolayers were washed three times with PBS and lysed in 1 mol/l NaOH solution. A 200 μl aliquot of the cell lysate was placed into a scintillation counter LS6000SC, Beckman Instruments, Fullerton, CA).

^{125}I-transferrin uptake was determined by a modification of the method published by Lamb et al. (14) incubating HMEC monolayers with 1 mg/ml ^{125}I-transferrin for 60 min at 37°C followed by stopping with 0.2 mol/l acetic acid.

Separation of cellular lipids by TLC

The incorporation of [^{3}H]oleate into cellular lipid pools was determined after incubation of 173 μmol/l [^{3}H]oleate-albumin (1:1, mol/mol) with HMEC monolayers as described above. Following lysis of HMEC by 1 mol/l NaOH, 0.6 ml of the cell lysate was mixed with 5.4 ml of chloroform-methanol (2:1, v/v) for the extraction of lipids according to Folch et al. (15). Aliquots of both the aqueous and lipid phases were counted to determine the recovery rate and water-soluble metabolites.

TLC was performed as described by Holehouse et al. (16) to separate specific classes of lipids. Standards of monoolein, diolein, triolein, cholesteryl oleate, free cholesterol, phosphatidylcholine, and free oleate were spotted onto silica gel plates at 10 μg per lane. The lipid phase obtained from the HMEC lysates was concentrated under a N_2 stream and spotted over the standards. The plates were developed in hexane-diethyl ether-acetic acid (80:20:1, v/v/v) to a height of 15 cm. Lipid standards were stained by I_2 vapor. The areas of each lane corresponding to lipid standards were scraped into a scintillation vial for measurement of radioactivity.

At least one control lane per plate contained lipid standards and cellular lipid extracts from cells incubated in medium without [^{3}H]oleate. Control lanes were scraped and counted to determine the background radioactivity for each lipid area and the mean background radioactivity was subtracted from individual lipid areas. The relative distribution of [^{3}H]oleate in specific cellular lipid classes was determined as the (lipid area cpm − mean backgroud cpm)/sum of cpm per lane.

Subcellular fractionation of HMEC by differential centrifugation

Cells from six petri dishes (ø 14 cm) were used for each preparation. HMEC were incubated with [^{3}H]oleate for 5 min as described above. All subsequent steps were carried out at 4°C. HMEC monolayers were washed three times in PBS, then scraped from the dishes and washed again three times in homogenization buffer (5 mmol/l Tris-HCl pH 7.4, 0.25 mol/l sucrose, 2 mmol/l $MgCl_2$) supplemented with DTT (1 mmol/l) and protease inhibitors (PMSF, 200 μg/ml; benzamidine, 0.5 mmol/l; leupeptin, 1 μg/ml). The cells were then resuspended in 10 ml homogenization buffer plus DTT/antiproteases and subjected to nitrogen cavitation (17, 18) for 15 min at 4°C at a pressure of 650 psi. The homogenate was centrifuged at 500 *g* for 15 min. Ribonuclease A (50 μg/ml) was added. After 30 min, the first differential centrifugation was carried out at 2,860 *g* (4,200 rpm in a Beckman JA20 rotor) for 10 min to obtain the mitochondrial pellet. The activity of cytochrome c oxidase was measured as described (19) to prove that mitochondria were enriched in this fraction. Recentrifugation of the remaining supernatant at 37,000 *g* (18,000 rpm in a Beckman JA12 rotor) yielded the peroxisome/plasma membrane pellet, as proven by measuring high activities of the marker enzymes catalase (20) and 5′-nucleotidase (Sigma, St. Louis, MO: kit no. 265B), respectively. The remaining supernatant was centrifuged at 100,000 *g* for 30 min to obtain the microsomal fraction containing endoplasmic reticulum (ER), Golgi membranes, caveolae, and clathrin-coated vesicles (CCV). All three pellets and the final supernatant after centrifugation of the microsomal pellet were subjected to liquid scintillation counting and Western blotting for clathrin and caveolin-1.

Confocal laser scanning microscopy

HMEC in chamber slides were incubated for 5 min with 80 μmol/l 12-NBD stearate and 80 μmol/l fatty acid-free BSA in PBS. Cells were washed three times with PBS and fixed in 2% paraformaldehyde. The first antibody was applied for 4 h at a dilution of 1:500 at 4°C followed by the second antibody for 2 h at 4°C diluted 1:500 in 0.05 mmol/l Tris-HCl, pH 7.4.

The L 310 microscope system (Zeiss, Oberkochen, Germany) was used for visualization. Individual cells were identified with a ×100 Plan-Neofluar multi-immersion objective (numerical aperture 0.9) by conventional light microscopy. The system was then switched to the frame mode and a confocal picture was generated with the argon laser (attenuation = 1). The depth of the optical section (confocal z resolution) was kept constant by holding the size of the aperture pinhole constant in the emission pathway.

Statistical analysis

Results are given as means ± SD. Student's *t*-test was used to test for significant differences among means. Linear and non-linear regression models were used to analyze the effect of free oleate concentration on the rate of initial uptake and to determine the mathematical model that best described the experimental data.

RESULTS

Uptake as a function of the external fatty acid concentration

The initial uptake of [^{3}H]oleate over 20 s was examined at various concentrations of free oleate in the incubation medium. The unbound oleate concentration was modulated without exceeding its solubility by mixing a fixed concentration of fatty acid-free BSA (173 μmol/l) with increasing concentrations of oleate (the oleate-albumin molar ratio varied between 0.1:1 up to 2:1). This provided a range of calculated unbound oleate concentrations of 6.5–429 μmol/l. With increasing concentrations of free oleate, the initial uptake followed a complex model with both linear and saturable components. The saturable component had a K_m of 25 ± 11 nmol/l and a V_{max} of 247 ± 50 pmol mg protein^{-1} min^{-1}. The slope of the linear component was 0.97 ± 0.13 l × mg protein^{-1} × min^{-1}(**Fig. 1**). The coefficient of determination was r^2 = 0.99 for this model. Thus, the initial influx of [^{3}H]oleate up to a concentration of 173 μmol/l (corresponding to a calculated concentration of 119 nmol/l unbound oleate) was for the most part mediated by the saturable component (Fig. 1) while with increasing concentrations the non-saturable, linear component became predominant (Fig. 1).

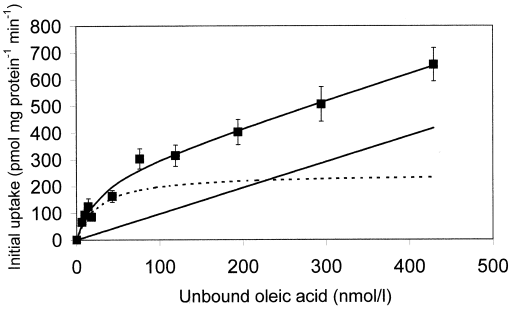

Fig. 1. Kinetics of initial influx. Initial influx of [^{3}H]oleate in human microvascular endothelial cells (HMEC) over 20 s as a function of the calculated concentrations of unbound oleate. Nonlinear statistical modeling showed that the data were best fit by a complex model with both linear (non-saturable, solid line) and nonlinear (saturable, dashed line) components. Data points are means ± SD of five replicate experiments.

Time dependence of [^{3}H]oleate uptake

The time course of [^{3}H]oleate uptake at a concentration of 173 μmol/l was linear over 40 s, representing ini-

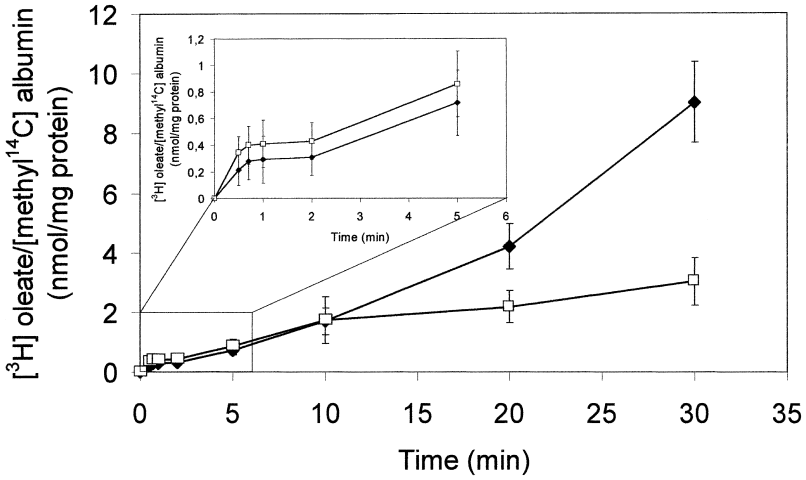

Fig. 2. Time dependence of [methyl-^{14}C]albumin and [^{3}H]oleate uptake in HMEC. HMEC monolayers were incubated with [^{3}H]oleate (closed diamonds) and [methyl-^{14}C]albumin (open squares) at an equimolar concentration of 173 μmol/l for periods lasting from 20 s to 30 min. Data are means ± SD of 10 replicate experiments.

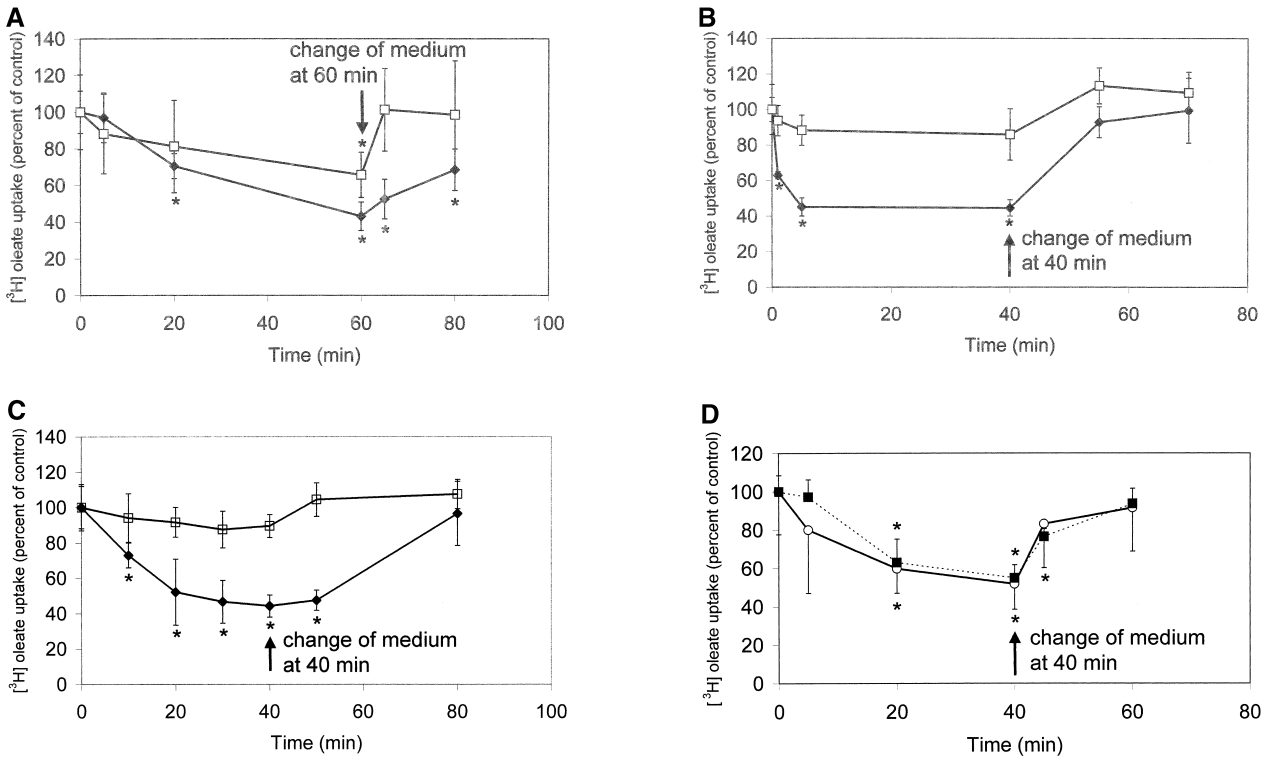

Fig. 3. Effect of pretreating HMEC with vesicle transport inhibitors on [^{3}H]oleate accumulation over 40 s and 5 min. HMEC were pretreated with inhibitors for the time periods indicated on the *x* axis. In order to test the reversibility of inhibitions, cells were washed and replenished with new medium containing no inhibitors at the time points indicated by the black arrows. The uptake of [^{3}H]oleate over 40 s (open squares) or 5 min (solid diamonds) was measured at all time points marked on the graphs, which show the percentage of [^{3}H]oleate accumulation compared to the controls (=100%). Data are means ± SD of 10 replicate experiments. The asterisks indicate statistical significance ($P < 0.05$). A: 30 μmol/l monensin. Absolute uptake in controls (= 100%): 1,716 ± 197 pmol/mg protein (5 min), 249 ± 61 pmol/mg protein (40 s). B: 2.5 μmol/l filipin III. Absolute uptake in controls (=100%): 1,347 ± 190 pmol/mg protein (5 min), 238 ± 49 pmol/mg protein (40 s). C: 10 mmol/l cyclodextrin. Absolute uptake in controls (=100%): 1,456 ± 260 pmol/mg protein (5 min), 271 ± 54 pmol/mg protein (40 s). D: Potassium-free medium (dotted line) or hypertonic medium (350 mmol/l NaCl) (solid line). Absolute uptake in controls (=100%): 1,613 ± 137 pmol/mg protein (5 min), 244 ± 61 pmol/mg protein (40 s).

tial influx and decreased thereafter (inset of **Fig. 2**). However, beyond 2 min of incubation, the time dependence of [^{3}H]oleate uptake revealed again a linear relationship over up to 30 min (Fig. 2). This indicates that the linear, non-saturable uptake component is a high capacity transport process that becomes predominant over time, while the saturable uptake component is a high affinity, low capacity process limited to the initial uptake over the first 40 s. In order to distinguish between these two components, [^{3}H]oleate uptake in the subsequent experiments was assessed over 40 s (representing the initial uptake predominantly mediated by the saturable component) and 5 min (predominantly mediated by the linear, non-saturable component).

Co-incubation of [methyl-^{14}C]albumin with [^{3}H]oleate

As LCFA are bound to albumin in the bloodstream as well as in our assay system, we compared the uptake rates of [methyl-^{14}C]albumin and [^{3}H]oleate finding that both were comparable within the first 10 min (Fig. 2). Thereafter, the accumulation of [^{3}H]oleate persistently increased over time in a linear fashion, while the net uptake of albumin appears to reach a steady state level (Fig. 2).

Effect of inhibitors on [^{3}H]oleate uptake in HMEC

Phloretin is a potent inhibitor of protein-mediated cellular transport systems, including the initial (saturable) uptake of LCFA by adipocytes (7). Pretreatment of HMEC with phloretin at a concentration of 400 μmol/l for 60 min reduced the initial uptake of [^{3}H]oleate (40 s) by 31.6 ± 13.1% while it did not affect [^{3}H]oleate uptake in the 5-min incubations. Thus, with increasing duration of [^{3}H]oleate accumulation, the contribution of the phloretin-sensitive, carrier-mediated uptake mechanism appears to decrease and eventually disappear.

As transport vesicles are abundant in endothelial cells, and [^{3}H]oleate uptake by a multitude of vesicles would be consistent with the linear component of the uptake kinetics, we next investigated the potential role of vesicular transport for [^{3}H]oleate uptake into HMEC.

NEM interferes with the fusion of transport vesicles and target membranes. By this mechanism, it inhibits intracellular transport by caveolae (21) as well as CCV (22). Pretreatment of HMEC with NEM at a concentration of 1 mmol/l for 90 s reduced [^{3}H]oleate accumulation by 34.4 ± 14.0% and 77.7 ± 1.7% in the 40-s and 5-min experiments, respectively.

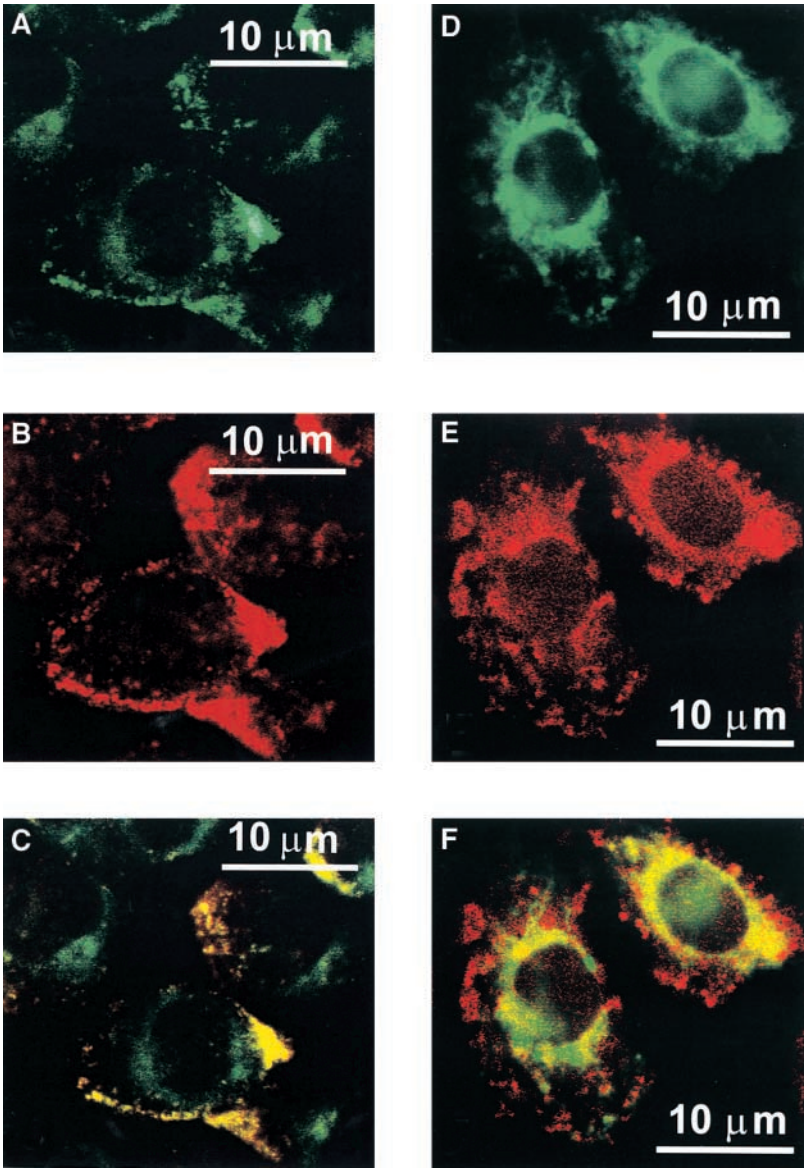

Fig. 4. Immunocytochemistry staining of caveolae and clathrin-coated vesicles (CCV) after 5 min of incubation with 12-(*N*-methyl)-*N*-[(7-nitrobenz-2-oxa-1,3-diazol-4-yl)amino]stearate (12-NBD). HMEC were incubated with 12-NBD stearate for 5 min, fixed, and prepared for analysis by microscopy (inverted Olympus IX50 system). A to C: Compare the distribution of 12-NBD stearate with staining of intracellular caveolae using a monoclonal antibody against caveolin-1: A: 12-NBD stearate B: Caveolin-1. C: Merge image demonstrating co-localization of 12-NBD stearate and caveolae in the subplasmalemmal section of the cell. D to F: Compare the distribution of 12-NBD stearate with staining of intracellular clathrin-coated vesicles (CCV) using a monoclonal antibody against clathrin heavy stain. D: 12-NBD stearate. E: Clathrin heavy chain. F: Merge image demonstrating co-localization of 12-NBD stearate and CCV in the perinuclear section of the cell.

Monensin inhibits vacuolar acidification (23), thus preventing receptor-ligand dissociation and recycling of the receptor to the cell surface. Receptor-mediated endocytosis is subsequently diminished as a cause of receptor trapping inside the cell (24). Monensin caused a reversible inhibition of [^{3}H]oleate uptake by 34.3% in the early and 56.9% in the late phase of oleate uptake (**Fig. 3A**).

These results indicate that vesicle-mediated transport is involved in [^{3}H]oleate uptake in HMEC and appears to play a larger role in the late uptake phase. However, the use of monensin or NEM does not distinguish between uptake by CCV and non-coated vesicles, i.e., caveolae. Therefore, we next used selective inhibitors of these different vesicular transport mechanisms.

Filipin III is a sterol-binding agent known to selectively disassemble endothelial noncoated vesicles (but not CCV), thus inhibiting caveolae-mediated intracellular transport in endothelial cells (25). Preincubation of HMEC with filipin III resulted in inhibition of [^{3}H]oleate uptake by 55.4% in the 5-min experiments (Fig. 3B). In contrast, its effect in the 40-s experiments was marginal (Fig. 3B), suggesting that caveolae might become operational in the

TABLE 1. Enzyme activities in HMEC fractions

	Cytochrome c Oxidase (Mitochondria)	Catalase (Peroxisomes)	Esterase (Microsomes)	5′-Nucleotidase (Plasma Membrane)
Mitochondria	49.4 ± 4.5	380 ± 170	1,206 ± 324	7.5 ± 4.9
Peroxisomes plasma membrane	17.6 ± 2.8	2,180 ± 350	1,016 ± 443	20.8 ± 9.5
Microsomes	2.8 ± 0.9	520 ± 280	1,860 ± 787	Not detectable

Fractions were obtained from HMEC lysates by differential centrifugation and analyzed for enzyme activities presented as units per gram total protein. Data are means ± SD of three experiments.

later phases of oleate uptake when the linear uptake component predominates. To corroborate this finding, we treated HMEC with cyclodextrin, another agent known to selectively inhibit caveolae by removing cholesterol from the plasma membrane (26, 27). As shown in Fig. 3C, the uptake of [^{3}H]oleic acid after preincubation with cyclodextrin for 40 min was only minimally affected at the 40 s time point, but reduced by 55.8% in the 5-min incubation experiments. In order to verify that both sterol-binding agents, filipin III and cyclodextrin, did not affect CCV in HMEC, we compared the uptake of ^{125}I-transferrin (which is endocytosed exclusively by CCV) in filipin III-treated or cyclodextrin-treated versus control HMEC and found no differences (data not shown).

Potassium depletion or hypertonicity (350 mmol/l NaCl) remove clathrin-coated pits from the plasma membrane in a reversible manner (28, 29) without affecting caveolae-mediated vesicular transport. In contrast to filipin III and cyclodextrin, these treatments reduced the uptake of [^{3}H]oleate into HMEC by 40–50% in both the early and late uptake phases (Fig. 3D). This effect was fully reversed within 20 min after repletion of K^+ or exchanging hypertonic with normotonic medium (Fig. 3D).

Visualization of 12-NBD stearate uptake by confocal LSM

In the presence of albumin, 12-NBD stearate was rapidly internalized into HMEC with pronounced staining of intracellular vesicles after 5 min (**Fig. 4A**, **D**). 12-NBD stearate accumulated particularly in perinuclear and subplasmalemmal sections without significantly staining the plasma membrane. Staining of intracellular vesicles with rhodamine-conjugated monoclonal antibodies against clathrin heavy chain (Fig. 4E) revealed co-localization of clathrin and 12-NBD stearate in the perinuclear sections of the cell (Fig. 4F). Staining with monoclonal antibodies against caveolin-1 demonstrated that caveolae vesicles are preferentially located in the subplasmalemmal sections of the cytoplasm (Fig. 4B), where co-localization with 12-NBD stearate was found (Fig. 4C). In summary, confocal LSM shows that both caveolae and CCV carry 12-NBD stearate, but in different subcellular locations of HMEC-1 cells.

Subcellular fractionation of HMEC lysates following [^{3}H]oleate uptake

Differential centrifugation was used to demonstrate enrichment of [^{3}H]oleate in partially purified vesicles. HMEC monolayers were treated with [^{3}H]oleate and subsequently fractionated to yield three fractions enriched in *a*) mitochondria, *b*) plasma membranes and peroxisomes, and *c*) microsomes including CCV and caveolae. Each fraction was characterized by a characteristic marker enzyme activity profile (30) (**Table 1**). Western blot analysis revealed strong clathrin and caveolin-1 bands in the microsomal pellet and weaker reactions in all other fractions (**Fig. 5**). As expected, [^{3}H]oleate was enriched in the microsomal fraction containing the majority of CCV and caveolae (**Fig. 6**).

Assessment of fluid-phase endocytosis in HMEC

Vesicle-mediated endocytosis may involve both specific receptor-mediated and non-selective fluid-phase endocytosis. Tritiated sucrose and dextran were used to quantitate fluid-phase endocytosis in HMEC and correlate it with oleate and albumin uptake. The uptake of [^{3}H]sucrose was 8-fold and of [^{3}H]dextran 5-fold less compared to [^{3}H]oleate independent of the incubation period (**Table 2**), showing that in HMEC there is only a minor contribution of fluid-phase endocytosis to total [^{3}H]oleate.

Intracellular metabolism of [^{3}H]oleate

A thorough analysis of intracellular oleate metabolism revealed that more than 75% were recovered unmetabolized from HMEC lysates within the first 10 min of incubation (**Table 3**). The remainder were found in various lipid

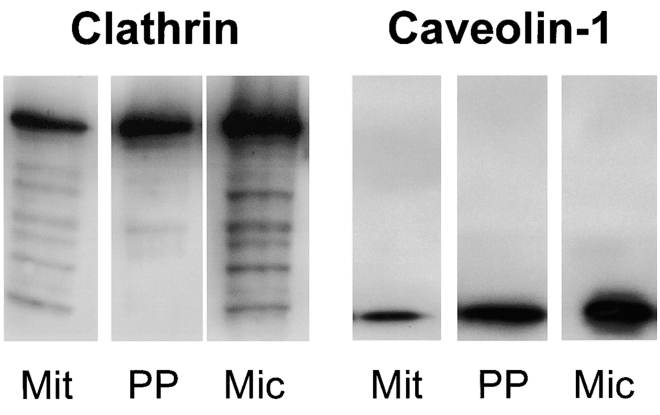

Fig. 5. Western blotting of subcellular HMEC fractions against caveolin-1 and clathrin. Equal protein amounts of three membranaceous fractions (Mit, mitochondrial; PP, plasma membrane/peroxisome; Mic, microsomal) were separated on an SDS gel, blotted to nitrocellulose, and probed for the presence of caveolin-1 or clathrin heavy chain using monoclonal antibodies.

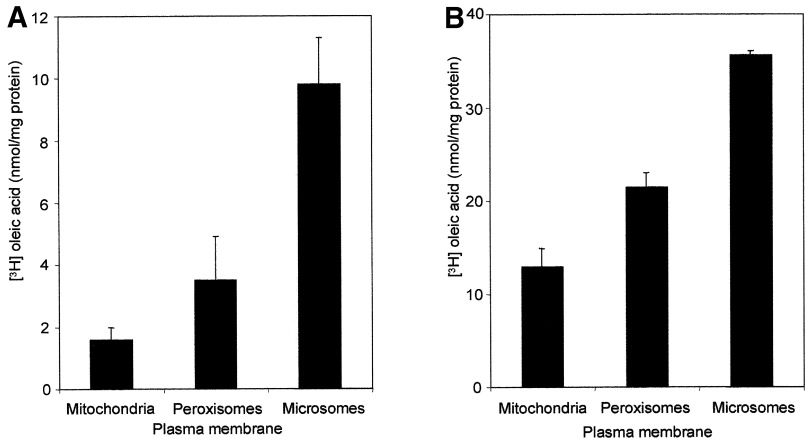

Fig. 6. Enrichment of [^{3}H]oleate in the microsomal fraction of HMEC. HMEC were treated with [^{3}H]oleate bound to albumin at 37°C for 40 s (A) and 5 min (B). Subsequently, the cells were lysed and fractionated as described in Materials and Methods. The fractions were enriched in (A) mitochondria, (B) peroxisomes and plasma membranes, and (C) microsomes (including clathrin-coated vesicles and caveolae). The values are means ± SD of three experiments.

classes (mono-, di-, and triglycerides, phospholipids and cholesteryl esters), each to a small degree (Table 3). $^{14}CO_2$ was not recovered from HMEC after 10 min of incubation with [^{3}H]oleate, however, ~0.1% of the total intracellular radioactivity was recovered as acid-soluble metabolites (data not shown).

In summary, intracellular metabolism of [^{3}H]oleate does not appear to play a major role in HMEC, indicating that LCFA are internalized into endothelial cells mainly for the purpose of shuttling them from the bloodstream to parenchymal cells that require LCFA as energy substrates.

DISCUSSION

In this study we present for the first time experimental data on the uptake of LCFA by HMEC supporting a model that involves both a low capacity protein-facilitated transport mechanism and a high capacity vesicle-mediated component involving both caveolae and CCV. The kinetic analysis demonstrated that the initial uptake of [^{3}H]oleate is a complex process involving a saturable and a linear component. The saturable component revealed a K_m of 25 ± 11 nmol/l and a V_{max} of 247 ± 50 pmol mg protein^{-1} min^{-1}. It is the predominant mechanism of initial [^{3}H]oleate uptake, suggesting the existence of a high affinity, low capacity carrier-mediated membrane translocation process. The K_m value of the saturable phase compares to that of other cell types as hepatocytes, cardiomyocytes, intestinal mucosal cells, or adipocytes (6–9). It is in line with the expectation that the K_m for carrier-mediated transfer of a particular substrate should be within the physiological concentration of this substrate. Circulating concentrations of LCFA have been reported to be in the 5–50 nanomolar range (31).

The linear uptake component represents a slow, low-affinity but high capacity transport system that after 2 min of incubation becomes the predominant factor in the overall uptake of LCFA by HMEC. The 5-min incubations were performed in our study in order to investigate this mechanism, which might theoretically rely on passive diffusion or simultaneous endocytosis by a multitude of vesicles (32). However, the different experimental approaches including biochemical inhibition of vesicular trafficking, immunofluorescence co-localization of 12-NBD stearate with vesicle proteins, and subcellular fractionation argue against passive diffusion and in favor of vesicle endocytosis involving both CCV and caveolae. Nonspecific fluid-phase endocytosis appears to be of minor

TABLE 2. Uptake rates of fluid phase endocytosis markers in HMEC compared to [^{3}H]oleate

Compound	Total Amount Offered in 2 ml Medium	Amount Internalized per mg Cell Protein		
		10 Min	20 Min	30 Min
[^{3}H]oleate	346 nmol (=100%)	4.12 ± 0.49 nmol (=1.2 ± 0.14%)	6.28 ± 0.34 nmol (=1.8 ± 0.1%)	9.02 ± 1.04 nmol (=2.6 ± 0.3%)
[^{3}H]sucrose	200 nmol (=100%)	0.31 ± 0.2 nmol (=0.16 ± 0.1%)	0.46 ± 0.11 nmol (=0.23 ± 0.06%)	0.57 ± 0.14 nmol (=0.29 ± 0.07%)
[^{3}H]dextran	10,000 μg (=100%)	26.8 ± 6.9 μg (=0.27 ± 0.07%)	35.9 ± 7.1 μg (=0.36 ± 0.07%)	55.3 ± 23.6 nmol (=0.55 ± 0.24%)

The relative values indicate which percentage of the total amount offered to the cells in 2 ml cell culture medium was internalized by the cells at 10, 20, and 30 min. HMEC, human microvascular endothelial cells.

TABLE 3. Intracellular metabolism of [^{3}H]oleate

	Counts/mg Protein	Percent
Total intracellular counts	49,257 ± 3,454	100 ± 7
Lipid (lower) phase	42,453 ± 3,668	86.2 ± 7.4
Aqueous (upper) phase	5,676 ± 310	11.5 ± 0.6
Not recovered	1,128 ± 612	2.3 ± 1.2
Distribution of [^{3}H]oleate in the lipid phase of HMEC lysates		
Total counts	35,020 ± 2,580	100 ± 7.4
Free oleate (R_f = 0.30)	30,730 ± 2,495	87.7 ± 7.0
Monoolein (R_f = 0.03)	1,146 ± 750	3.3 ± 2.1
Diolein (R_f = 0.20)	537 ± 394	1.5 ± 1.1
Triolein (R_f = 0.73)	621 ± 415	1.8 ± 1.2
Cholesteryl ester (R_f = 0.87)	436 ± 349	1.2 ± 1.0
Phospholipids (PE, PS) (R_f = 0.62)	865 ± 682	2.5 ± 1.9
Unidentified	685 ± 608	2.0 ± 1.7

For these assays, HMEC-1 cell monolayers were incubated in serum-free medium with 173 μmol/oleate plus [^{3}H]oleate tracer bound to 173 μmol/l albumin for 10 min. HMEC were lysed followed by extraction of the lysate according to Folch et al. (15). The lipid phase was separated by TLC using hexane-diethyl ether-acetic acid (80:20:1, v/v/v) as developing solvent. Areas of the TLC plates corresponding to lipid standards were removed for scintillation counting. All spots were counted and the counts were totaled. The percentage of [^{3}H]oleate in lipid classes was calculated as (lipid area cpm − mean backgroud cpm)/sum of cpm per lane. Since the solvent front was allowed to reach the upper edge of the TLC plate, the R_f values were calculated using the distance from the origin to the upper edge of the plate as the denominator. The dioleyl-phosphatidylethanolamine (PE) and dioleyl-phosphatidylserine (PS) standards were summarized as "phospholipids" since both had an identical R_f value in this TLC system. Note that oleyl-CoA moieties were not recovered by this assay, as they were invariably lost by the extraction and N_2 evaporation procedures. Data are means ± SD of five replicate experiments.

significance, as only a calculated portion of 10–20% of the total [^{3}H]oleate uptake could be attributed to this mechanism using radiolabeled dextran and sucrose.

Caveolae are 50–100 nm flask-shaped invaginations of the plasma membrane that have an endocytotic function (potocytosis and transcytosis) akin to that of CCV, albeit with different substrate specificities and via different mechanisms of trafficking (33). Both CCV and caveolae play a crucial role in the inward and outward cellular cholesterol transport (34) and target their incorporated cargo to various intracellular pathways or transcellular traffic from the apical (luminal) to the basolateral (parenchymal) side of endothelial cells (21, 25). Caveolae harbor a specific set of membrane proteins that can bind and transport hydrophobic molecules like fatty acids and cholesterol. CD36/fatty acid translocase (FAT), a protein that is involved in fatty acid uptake (35), and scavenger receptor class B type I, a receptor that mediates selective uptake of cholesterol esters, reside in caveolae (36, 37). Caveolin-1 itself binds fatty acids with high affinity (38, 39) and has a well characterized function in regulation of influx and efflux of cholesterol (34, 40–42). In addition, we recently reported that caveolae are involved in LCFA uptake and intracellular trafficking by HepG2 hepatoma cells (43). The data reported here establish that this mechanism is not restricted to hepatocytes, and that in addition to caveolae, CCV are as well capable of transporting LCFA. Indeed, the inhibition of [^{3}H]oleate uptake in the early phase by inhibitors of CCV but not caveolae suggests that CCV might become operational in LCFA uptake before caveolae.

LCFA must interact with the endothelial cell plasma membrane prior to their incorporation into CCV or caveolae. It is currently unknown if LCFA directly bind to plasma membrane proteins with high affinity for fatty acids (e.g., CD36/FAT, caveolin-1, or fatty acid transport protein-1) or if they bind to albumin receptor sites as LCFA-albumin complexes. The first mechanism would require dissociation from albumin prior to receptor binding. The latter option is supported by our observation that [methyl-^{14}C]albumin was taken up by HMEC at equimolar amounts compared to [^{3}H]oleate within the first 10 min. This is in accordance with the observation of Galis et al. (44), who showed that albumin-LCFA complexes are taken up by intracellular vesicles of lung endothelial cells with higher affinity than defatted albumin. These authors suggested that conformational changes of albumin (e.g., by LCFA binding) might modify the interaction with a putative endothelial cell receptor, resulting in enhanced vesicular uptake and transcytosis. The discrepancy between the net accumulation of [^{3}H]oleate versus [methyl-^{14}C]albumin at the time points later than 10 min (Fig. 2) might be due to recycling of albumin back to the extracellular space following intracellular dissociation from LCFA. This possibility needs to be investigated in the future using double chamber culture systems allowing determination of transcytosis and recycling (45).

In summary, the initial (40 s) uptake phase may include binding of free LCFA to membrane fatty acid binding proteins or LCFA-albumin complexes to putative albumin receptor sites, and the formation of CCV. In the later phase of uptake, the steady maintenance of an extensive pool of transport vesicles, CCV as well as caveolae, may subsequently sustain the uptake of large amounts of LCFA over time.

Subcellular fractionation was performed in order to purify CCV and caveolae based on the methods used by Fielding and Fielding (34) and Bradbury et al. (46). These authors obtained a microsomal fraction containing CCV and caveolae by differential centrifugation of fibroblasts (34) or T84 intestinal cells (46). In the present study, [^{3}H]oleate was found concentrated in this microsomal fraction following uptake by HMEC (Fig. 6). This suggests shuttling of LCFA towards the microsomal fraction, which was enriched in CCV and caveolae, was assessed by Western blotting against the respective marker proteins clathrin heavy chain and caveolin-1. Besides these transport vesicles, the microsomal fraction as well contains ER and Golgi membranes, to which some [^{3}H]oleate might be targeted for subsequent metabolic disposition. However, thorough analysis revealed that LCFA metabolism does not play a major role in HMEC, as >75% of intracellular oleate remained unmetabolized within 10 min. This concurs with Spahr et al. (47), who showed that coronary microvascular endothelial cells do not depend on fatty acids as energy source. Nagelkerke et al. (5) describe that native oleate is almost instantaneously transferred from

liver endothelial to parenchymal cells, which then reutilize the fatty acid for the synthesis of phospholipids and triacylglycerols. Thus, endothelial cells appear to act as LCFA providers organizing the transit of native LCFA from the bloodstream to the underlying parenchymal cells. The determination of LCFA transcytosis across HMEC monolayers awaits further study using double chamber culture systems (45).

In summary, our data indicate that LCFA uptake in HMEC consists of both a low-capacity protein-facilitated transport mechanism operational in the early uptake phase followed by a novel high capacity mechanism of LCFA traffic through caveolae and CCV that becomes predominant in the later uptake phase.

This work was supported by grant Str 216/11-1 from the Deutsche Forschungsgemeinschaft and a Dietmar Hopp Stiftung grant to W.S.

REFERENCES

1. Van der Vusse, G. J., J. F. C. Glatz, F. A. van Nieuwenhoven, R. S. Reneman, and J. B. Bassingthwaighte. 1998. Transport of long-chain fatty acids across the muscular endothelium. *In* Skeletal muscle metabolism in exercise and diabetes. 441. E. A. Richter, H. Galbo, B. Kiens, and B. Saltin, editors. Plenum Press, New York, NY. 181-191.
2. Yamashita, A., T. Suguira, and K. Waku. 1997. Acyltransferases and transacylases involved in fatty acid remodeling of phospholipids and metabolism of bioactive lipids in mammalian cells. *J. Biochem.* **122:** 1–16.
3. Van den Heuvel, J. P. 1999. Peroxisome proliferator-activated receptors: a critical link among fatty acids, gene expression and carcinogenesis. *J. Nutr.* **129 (Suppl.)**: 575S–580S.
4. Weisiger, R. A., and W. L. Ma. 1987. Uptake of oleate from albumin solutions by rat liver. Failure to detect catalysis of the dissociation of oleate from albumin by an albumin receptor. *J. Clin. Invest.* **79:** 1070–1077.
5. Nagelkerke, J. F., and T. J. van Berkel. 1986. Rapid transport of fatty acids from rat liver endothelial to parenchymal cells after uptake of cholesteryl ester-labeled acetylated LDL. *Biochim. Biophys. Acta.* **875:** 593–598.
6. Stremmel, W., G. Strohmeyer, and P. D. Berk. 1986. Hepatocellular uptake of oleate is energy dependent, sodium linked, and inhibited by an antibody to a hepatocyte plasma membrane fatty acid binding protein. *Proc. Natl. Acad. Sci. USA.* **83:** 3584–3588.
7. Abumrad, N. A., R. C. Perkins, J. H. Park, and C. R. Park. 1981. Mechanism of long chain fatty acid permeation in the isolated adipocyte. *J. Biol. Chem.* **256:** 9183–9191.
8. Stremmel, W. 1988. Fatty acid uptake by isolated rat heart myocytes represents a carrier-mediated transport process. *J. Clin. Invest.* **81:** 844–852.
9. Goré, J., and C. Hoinard. 1993. Linolenic acid transport in hamster intestinal cells is carrier-mediated. *J. Nutr.* **123:** 66–73.
10. Ades, E. W., F. J. Candal, R. A. Swerlick, V. G. George, S. Summers, D. C. Bosse, and T. J. Lawley. 1992. HMEC-1: establishment of an immortalized human microvascular endothelial cell line. *J. Invest. Dermatol.* **99:** 683–690.
11. Pruckler, J. M., T. J. Lawley, and E. W. Ades. 1993. Use of a human microvascular endothelial cell line as a model system to evaluate cholesterol uptake. *Pathobiology.* **61:** 283–287.
12. Wosilait, W. D., and P. Nagy. 1976. A method of computing drug distribution in plasma using stepwise association constants: clofibrate acid as an illustrative example. *Comput. Programs Biomed.* **6:** 142–148.
13. Spector, A. A., J. E. Fletcher, and J. D. Ashbrook. 1971. Analysis of long-chain free fatty acid binding to bovine serum albumin by determination of stepwise equilibrium constants. *Biochemistry.* **10:** 3229–3232.
14. Lamb, J. E., F. Ray, J. H. Ward, J. P. Kushner, and J. Kaplan. 1993. Internalization and subcellular localization of transferrin and transferrin receptors in HeLa cells. *J. Biol. Chem.* **258:** 8751–8758.
15. Folch, J., M. B. Lees, and G. H. S. Stanley. 1957. A simple method for isolation and purification of total lipids from animal tissues. *J. Biol. Chem.* **226:** 497–509.
16. Holehouse, E. L., M. L. Liu, and G. W. Aponte. 1998. Oleate distribution in small intestinal epithelial cells expressing intestinal-fatty acid binding protein. *Biochim. Biophys. Acta.* **1390:** 52–64.
17. Gottlieb, R. A., and S. Adachi. 2000. Nitrogen cavitation for cell disruption to obtain mitochondria from cultured cells. *Methods Enzymol.* **322:** 213–221.
18. Teitel, J. M. 1986. Specific inhibition of endothelial cell proliferation by isolated endothelial plasma membranes. *J. Cell. Physiol.* **128:** 329–336.
19. Van den Heuvel, J.P. 1999. Peroxisome proliferator-activated receptors: a critical link among fatty acids, gene expression and carcinogenesis. *J. Nutr.* **129 (Suppl)**: 575S–580S.
20. Völkl, A., and H. D. Fahimi. 1985. Isolation and characterization of peroxisomes from the liver of normal untreated rats. *Eur. J. Biochem.* **149:** 257–265.
21. Schnitzer, J. E., J. Allard, and P. Oh. 1995. NEM inhibits transcytosis, endocytosis, and capillary permeability: implication of caveolae fusion in endothelia. *Am. J. Physiol.* **268:** H48–H55.
22. Steel, G. J., M. Tagaya, and P. G. Woodman. 1996. Association of the fusion protein NSF with clathrin-coated vesicle membranes. *EMBO J.* **15:** 745–752.
23. Conte, M. P., G. Petrone, C. Longhi, P. Valenti, R. Morelli, F. Superti, and L. Seganti. 1996. The effects of inhibitors of vacuolar acidification on the release of *Listeria monocytogenes* from phagosomes of Caco-2 cells. *J. Med. Microbiol.* **44:** 418–424.
24. Hastings, R. H., J. R. Wright, K. H. Albertine, R. Ciriales, and M. A. Matthay. 1994. Effect of endocytosis inhibitors on alveolar clearance of albumin, immunoglobulin G, and SP-A in rabbits. *Am. J. Physiol.* **266:** L544–L552.
25. Schnitzer, J. E., P. Oh, E. Pinney, and J. Allard. 1994. Filipin-sensitive caveolae-mediated transport in endothelium: reduced transcytosis, scavenger endocytosis, and capillary permeability of select macromolecules. *J. Cell Biol.* **127:** 1217–1232.
26. Fitz, J. G., N. M. Bass, and R. A. Weisiger. 1991. Hepatic transport of a fluorescent stearate derivative: electrochemical driving forces in intact rat liver. *Am. J. Physiol.* **261:** G83–G91.
27. Bass, N. M. 1988. The cellular fatty acid binding proteins: aspects of structure, regulation, and function. *Int. Rev. Cytol.* **111:** 143–184.
28. Cupers, P., A. Veithen, A. Kiss, P. Baudhuin, and P. J. Courtoy. 1994. Clathrin polymerization is not required for bulk-phase endocytosis in rat fetal fibroblasts. *J. Cell Biol.* **127:** 725–735.
29. Altankov, G., and F. Grinnell. 1993. Depletion of intracellular potassium disrupts coated pits and reversibly inhibits cell polarization during fibroblast spreading. *J. Cell Biol.* **120:** 1449–1459.
30. Völkl, A., and H. D. Fahimi. 1985. Isolation and characterization of peroxisomes from the liver of normal untreated rats. *Eur. J. Biochem.* **149:** 257–265.
31. Richieri, G. V., and A. M. Kleinfeld. 1995. Unbound free fatty acid levels in human serum. *J. Lipid Res.* **36:** 229–240.
32. Tibaduiza, E. C., and D. Bobilya. 1996. Zinc transport across an endothelium includes vesicular cotransport with albumin. *J. Cell. Physiol.* **167:** 539–547.
33. Ostrom, R. S., and P. Insel. 1999. Caveolar microdomains of the sarcolemma: compartmentation of signaling molecules comes of age (editorial). *Circ. Res.* **84:** 1110–1112.
34. Fielding, P. E., and C. J. Fielding. 1996. Intracellular transport of low density lipoprotein derived free cholesterol begins at clathrin-coated pits and terminates at cell surface caveolae. *Biochemistry.* **35:** 14932–14938.
35. Abumrad, N. A., M. R. El-Maghrabi, E. Z. Amri, E. Lopez, and P. A. Grimaldi. 1993. Cloning of a rat adipocyte membrane protein implicated in binding or transport of long-chain fatty acids that is induced during preadipocyte differentiation. Homology with human CD36. *J. Biol. Chem.* **268:** 17665–17668.
36. Babitt, J., B. Trigatti, A. Rigotti, E. J. Smart, R. G. Anderson, S. Xu, and M. Krieger. 1997. Murine SR-BI, a high density lipoprotein receptor that mediates selective lipid uptake, is *N*-glycosylated and fatty acylated and colocalizes with plasma membrane caveolae. *J. Biol. Chem.* **272:** 13242–13249.
37. Malerød, L., L. K. Juvet, T. Gjøen, and T. Berg. 2002. The expression of scavenger receptor class B, type I (SR-BI) and caveolin-1 in

parenchymal and nonparenchymal liver cells. *Cell Tissue Res.* **307:** 173–180.
38. Trigatti, B., R. G. Anderson, and G. E. Gerber. 1999. Identification of caveolin-1 as a fatty acid binding protein. *Biochem. Biophys. Res. Commun.* **255:** 34–39.
39. Gerber, G. E., D. Mangroo, and B. L. Trigatti. 1993. Identification of high affinity membrane-bound fatty acid-binding proteins using a photoreactive fatty acid. *Mol. Cell. Biochem.* **123:** 39–44.
40. Conrad, P. A., E. J. Smart, Y. S. Ying, R. G. W. Anderson, and G. S. Bloom. 1995. Caveolin cycles between plasma membrane caveolae and the Golgi complex by microtubule-dependent and microtubule-independent steps. *J. Cell Biol.* **131:** 1421–1433.
41. Hailstones, D., L. S. Sleer, R. G. Parton, and K. K. Stanley. 1998. Regulation of caveolin and caveolae by cholesterol in MDCK cells. *J. Lipid Res.* **39:** 369–379.
42. Smart, E. J., Y. S. Ying, P. A. Conrad, and R. G. W. Anderson. 1994. Caveolin moves from caveolae to the golgi apparatus in response to cholesterol oxidation. *J. Cell Biol.* **127:** 1185–1197.
43. Pohl, J., A. Ring, and W. Stremmel. 2002. Uptake of long-chain fatty acids in HepG2 cells involves caveolae: analysis of a novel pathway. *J. Lipid Res.* **43:** 1390–1399.
44. Galis, Z., L. Ghitescu, and M. Simionescu. 1988. Fatty acids binding to albumin increases its uptake and transcytosis by the lung capillary endothelium. *Eur. J. Cell Biol.* **47:** 358–365.
45. Ring, A., J. N. Weiser, and E. I. Tuomanen. 1998. Pneumococcal trafficking across the blood-brain barrier: molecular analysis of a novel bi-directional pathway. *J. Clin. Invest.* **102:** 347–360.
46. Bradbury, N. A., J. A. Cohn, C. J. Venglarik, and R. J. Bridges. 1994. Biochemical and biophysical identification of cystic fibrosis transmembrane conductance regulator chloride channels as components of endocytic CCV. *J. Biol. Chem.* **269:** 8296–8302.
47. Spahr, R., A. Krutzfeldt, S. Mertens, S. Siegmund, and H. M. Piper. 1989. Fatty acids are not an important fuel for coronary microvascular endothelial cells. *Mol. Cell. Biochem.* **88:** 59–64.